# Investigating phase portraits and extraction of new solitary wave solutions related to the generalized resonant nonlinear Schrödinger equation

A. Rashid Butt
*Department of Mathematics, University of Engineering and Technology, Lahore, Pakistan.*

F. Bashir Farooq
*Department of Mathematics and Statistics, College of Science,*
*Imam Mohammad Ibn Saud Islamic University (IMSIU), Saudia Arabia.*

N. Akram
*Department of Mathematics, University of Engineering and Technology, Lahore, Pakistan.*

N. Raza
*Institute of Mathematics, University of the Punjab, Lahore, Pakistan.*
*Mathematics Research Center, Near East University, Near East Boulevard, Nicosia, Mersin 10, Turkey.*

Received 28 October 2022; accepted 2 September 2024

This research dissects solitary wave solutions of the generalized resonant nonlinear Schrödinger equation, whose primary uses include the transmission of light across nonlinear optical fibers. To generate bright, dark, kink-type, and singular kink-type solitary waves that rely on the intensity of the propagating pulse, an extended direct algebraic technique with symbolic computation is used. For different values of the parameters, the propagation of some specific solutions in a graphically detailed report has also been demonstrated. Then the bifurcation structures of the heeded model have been determined using a planar dynamical system and phase portraits.

*Keywords:* Resonant nonlinear Schrödinger equation; solitary waves; optical solitons; extended direct algebraic method.

DOI: https://doi.org/10.31349/RevMexFis.71.031301

## 1. Introduction

The study of optical solitons is one of the most significant fields of investigation in nonlinear optics, particularly in media transmission design and hypothetical material science. Hypothetical material science is the study of theoretical and unproven materials not yet discovered or synthesized, using advanced computational methods to predict their properties and potential applications. It aims to explore new possibilities for materials that could revolutionize various technologies [1,2]. In fiber optics and nonlinear waveguides, analyzing optical solitons is truly unavoidable. They are crucial in optical continuum synthesis and can be used to convey information across enormously long distances [3-6]. Besides that, a detailed analysis of the majority of optical fibers and their networks usually demands a number of complex mechanisms that influence the dynamics of the system. Optical fibers transmit data as light pulses for high-speed communication. These fibers have a core and cladding with different refractive indices, enabling efficient data transmission over long distances with minimal loss. The fundamental optical solitons reported in these processes is generic from the nonlinear Schrödinger equations (NLSEs).

NLSEs are nonlinear partial differential equations in dispersive form that have been generated and examined in a variety of nonlinear domains, such as discrete spatial optical solitons in waveguide arrays and quasi-stationary optical solitons with parabolic law nonlinearity [7,8]. The fact that these equations represent the modeling of numerous fundamental phenomena, including DNA structure modeling, wave dynamics in optical fibers, and wave pattern production in semiconductor materials, demonstrates their relevance in scientific and technological advancements. Many additional scholars have investigated these systems using other approaches such as the new $\phi^6-$model expansion method [9], the $\exp(-\phi(X))-$expansion, the first integral method and the $G^{'}/G^2-$expansion [10,11], the extended trial approach [12], the generalized auxiliary equation technique [13], the $\tanh$ method [14], and the extended form of simple equation method [15]. The study of generalized NLSEs that account for resonant phenomena has sparked significant attention. In this article, we have resolved the generalized resonant nonlinear Schrödinger equation with an arbitrary index,

$$\mathrm{i}\phi_t + a\phi_{xx} + (\alpha|\phi|^{2n} + \beta|\phi|^{4n})\phi + \delta\left(\frac{|\phi|_{xx}}{|\phi|}\right)\phi - \epsilon\phi = 0, \tag{1}$$

where $\phi = \phi(x,t)$ represents the complex-valued function, $x$ is the adimensional length along the fiber, $t$ represents time, $\epsilon$ is a parameter, $\alpha$ and $\beta$ are the coefficients of the Kerr law nonlinearity, $a$ the group velocity dispersion (GVD), $\delta$ is the resonant nonlinearity, and $n$ is an arbitrary index $(n \neq 0, -1)$.

However, as far as we know, not all solutions for this specific form of the equation have been discovered. Multiple authors have tried to find the solution of other forms of resonant nonlinear Schrödinger equation with specific indicators of the reflection coefficient [16-21]. Regarding this spacial form of the equation, we are interested in examining whether these solutions remain stable when parameters vary. To gain a deeper understanding of the soliton dynamics within this model, we aim to study its solutions for arbitrary index and their stability with respect to parameter changes. Only few articles have dealt with this special equation form. In Ref. [22] the author used the Jacobi elliptic sine method to find general solutions. On the other hand, in Ref. [23] the Bernoulli sub-ODE method and the $(G^{'}/G)-$expansion method have been used to study the behavior of the model. It is self-evident that this model is a non-integrable partial differential equation, and the inverse scattering transform cannot generate a solution for this problem. Hence, the extended direct algebraic technique plus bifurcation analysis have been used to explore new structures of the governing model. These methods are effectively applied to study various nonlinear problems and can also be used for qualitative analysis and to discuss the stability of solutions with respect to parameter changes.

The framework of this research is as follows: In Sec. 2 extended direct algebraic method is elaborated. In Sec. 3 application of the technique on the considered equation and graphical representation can be seen. In Sec. 4, bifurcation analysis and phase portrait of the heeded model are described. The conclusion of the work is summarized in Sec. 5.

## 2. Recapitulation of the presented technique

These are the core steps to demonstrate the primary aspects of the extended direct algebraic method [24-27].

**Step 1:** Consider the nonlinear partial differential equation (NLPDE) of the form:

$$D(\phi, \phi_t, \phi_x, \phi_{tt}, \phi_{xx}, ...) = 0, \tag{2}$$

where $\phi = \phi(x, t)$ is a function to be determined. Consider the following traveling wave transformation [28,29]:

$$\begin{aligned}\phi(x,t) &= \exp(\mathrm{i}\xi) W(\eta), \qquad \xi = d_1 x - c_1 t,\\ \eta &= d_2 x - c_2 t,\end{aligned} \tag{3}$$

where, $d_1$, $d_2$ are the arbitrary constants and $c_1$, $c_2$ are the speed and the phase of the travelling wave respectively. Now, using this transformation in Eq. (2) we had the following standard ordinary differential equation:

$$d(W, W^{'}, W^{''}, ...) = 0, \tag{4}$$

where $d$ is the polynomial in $W(\eta)$ and its derivatives.

**Step 2:** Suppose Eq. (4) has solution of the form:

$$W(\eta) = \sum_{i=0}^{N} \left[ b_i B(\eta)^i \right], \tag{5}$$

with $B(\eta)$ satisfies following ODE,

$$B'(\eta) = \ln(\rho)\left(\mu + \nu B(\eta) + \zeta B^2(\eta)\right), \quad \rho \neq 0, 1. \tag{6}$$

Here, $\rho$ is a positive integer. For $\Theta = (\nu^2 - 4\mu\zeta)$ the solutions of Eq. (6) expressed in terms of parameters $\mu$, $\nu$ and $\zeta$ are as follows:

**1:** If $\Theta < 0$ and $\zeta \neq 0$,

$$B_1(\eta) = -\frac{\nu}{2\zeta} + \frac{\sqrt{-\Theta}}{2\zeta} \tan_\rho\left(\frac{\sqrt{-\Theta}}{2}\eta\right), \tag{7}$$

$$B_2(\eta) = -\frac{\nu}{2\zeta} - \frac{\sqrt{-\Theta}}{2\zeta} \cot_\rho\left(\frac{\sqrt{-\Theta}}{2}\eta\right), \tag{8}$$

$$B_3(\eta) = -\frac{\nu}{2\zeta} + \frac{\sqrt{-\Theta}}{2\zeta}\Bigg( \tan_\rho(\sqrt{-\Theta}\eta) \pm \sqrt{pq}\sec_\rho(\sqrt{-\Theta}\eta)\Bigg), \tag{9}$$

$$B_4(\eta) = -\frac{\nu}{2\zeta} + \frac{\sqrt{-\Theta}}{2\zeta}\Bigg( \cot_\rho(\sqrt{-\Theta}\eta) \pm \sqrt{pq}\csc_\rho(\sqrt{-\Theta}\eta)\Bigg), \tag{10}$$

$$B_5(\eta) = -\frac{\nu}{2\zeta} + \frac{\sqrt{-\Theta}}{4\zeta}\Bigg( \tan_\rho(\frac{\sqrt{-\Theta}}{4}\eta) - \cot_\rho(\frac{\sqrt{-\Theta}}{4}\eta)\Bigg). \tag{11}$$

**2:** If $\Theta > 0$ and $\zeta \neq 0$,

$$B_6(\eta) = -\frac{\nu}{2\zeta} - \frac{\sqrt{\Theta}}{2\zeta} \tanh_\rho\left(\frac{\sqrt{\Theta}}{2}\eta\right), \tag{12}$$

$$B_7(\eta) = -\frac{\nu}{2\zeta} - \frac{\sqrt{\Theta}}{2\zeta} \coth_\rho\left(\frac{\sqrt{\Theta}}{2}\eta\right), \tag{13}$$

$$B_8(\eta) = -\frac{\nu}{2\zeta} + \frac{\sqrt{\Theta}}{2\zeta}\Big( -\tanh_\rho(\sqrt{\Theta}\eta) \pm \mathrm{i}\sqrt{pq}\,\mathrm{sech}_\rho(\sqrt{\Theta}\eta)\Big), \tag{14}$$

$$B_9(\eta) = -\frac{\nu}{2\zeta} + \frac{\sqrt{\Theta}}{2\zeta}\left(-\coth_\rho\left(\sqrt{\Theta}\eta\right) \pm \sqrt{pq}\,\mathrm{csch}_\rho\left(\sqrt{\Theta}\eta\right)\right), \tag{15}$$

$$B_{10}(\eta) = -\frac{\nu}{2\zeta} - \frac{\sqrt{\Theta}}{4\zeta}\left(\tanh_\rho\left(\frac{\sqrt{\Theta}}{4}\eta\right) + \coth_\rho\left(\frac{\sqrt{\Theta}}{4}\eta\right)\right). \tag{16}$$

**3:** If $\mu\zeta > 0$ and $\nu = 0$,

$$B_{11}(\eta) = \sqrt{\frac{\mu}{\zeta}}\tan_\rho\left(\sqrt{\mu\zeta}\eta\right), \tag{17}$$

$$B_{12}(\eta) = -\sqrt{\frac{\mu}{\zeta}}\cot_\rho\left(\sqrt{\mu\zeta}\eta\right), \tag{18}$$

$$B_{13}(\eta) = \sqrt{\frac{\mu}{\zeta}}\left(\tan_\rho\left(2\sqrt{\mu\zeta}\eta\right) \pm \sqrt{pq}\sec_\rho\left(2\sqrt{\mu\zeta}\eta\right)\right), \tag{19}$$

$$B_{14}(\eta) = \sqrt{\frac{\mu}{\zeta}}\left(-\cot_\rho\left(2\sqrt{\mu\zeta}\eta\right) \pm \sqrt{pq}\csc_\rho\left(2\sqrt{\mu\zeta}\eta\right)\right), \tag{20}$$

$$B_{15}(\eta) = \frac{1}{2}\sqrt{\frac{\mu}{\zeta}}\left(\tan_\rho\left(\frac{\sqrt{\mu\zeta}}{2}\eta\right) - \cot_\rho\left(\frac{\sqrt{\mu\zeta}}{2}\eta\right)\right). \tag{21}$$

**4:** If $\mu\zeta < 0$ and $\nu = 0$,

$$B_{16}(\eta) = -\sqrt{-\frac{\mu}{\zeta}}\tanh_\rho\left(\sqrt{-\mu\zeta}\eta\right), \tag{22}$$

$$B_{17}(\eta) = -\sqrt{-\frac{\mu}{\zeta}}\coth_\rho\left(\sqrt{-\mu\zeta}\eta\right), \tag{23}$$

$$B_{18}(\eta) = \sqrt{-\frac{\mu}{\zeta}}\left(-\tanh_\rho\left(2\sqrt{-\mu\zeta}\eta\right) \pm \mathrm{i}\sqrt{pq}\,\mathrm{sech}_\rho\left(2\sqrt{-\mu\zeta}\eta\right)\right), \tag{24}$$

$$B_{19}(\eta) = \sqrt{-\frac{\mu}{\zeta}}\left(-\coth_\rho\left(2\sqrt{-\mu\zeta}\eta\right) \pm \sqrt{pq}\,\mathrm{csch}_\rho\left(2\sqrt{-\mu\zeta}\eta\right)\right), \tag{25}$$

$$B_{20}(\eta) = -\frac{1}{2}\sqrt{-\frac{\mu}{\zeta}}\left(\tanh_\rho\left(\frac{\sqrt{-\mu\zeta}}{2}\eta\right) + \coth_\rho\left(\frac{\sqrt{-\mu\zeta}}{2}\eta\right)\right). \tag{26}$$

**5:** If $\nu = 0$ and $\mu = \zeta$,

$$B_{21}(\eta) = \tan_\rho(\mu\eta), \tag{27}$$

$$B_{22}(\eta) = -\cot_\rho(\mu\eta), \tag{28}$$

$$B_{23}(\eta) = \tan_\rho(2\mu\eta) \pm \sqrt{pq}\sec_\rho(2\mu\eta), \tag{29}$$

$$B_{24}(\eta) = -\cot_\rho(2\mu\eta) \pm \sqrt{pq}\csc_\rho(2\mu\eta), \tag{30}$$

$$B_{25}(\eta) = \frac{1}{2}\left(\tan_\rho\left(\frac{\mu}{2}\eta\right) - \cot_\rho\left(\frac{\mu}{2}\eta\right)\right). \tag{31}$$

**6:** If $\nu = 0$ and $\zeta = -\mu$,

$$B_{26}(\eta) = -\tanh_\rho(\mu\eta), \tag{32}$$

$$B_{27}(\eta) = -\coth_\rho(\mu\eta), \tag{33}$$

$$B_{28}(\eta) = -\tanh_\rho(2\mu\eta) \pm \sqrt{-pq}\,\mathrm{sech}_\rho(2\mu\eta), \tag{34}$$

$$B_{29}(\eta) = -\coth_\rho(2\mu\eta) \pm \sqrt{pq}\,\mathrm{csch}_\rho(2\mu\eta), \tag{35}$$

$$B_{30}(\eta) = -\frac{1}{2}\left(\tanh_\rho\left(\frac{\mu}{2}\eta\right) + \coth_\rho\left(\frac{\mu}{2}\eta\right)\right). \tag{36}$$

**7:** If $\Theta = 0$,

$$B_{31}(\eta) = \frac{-2\mu(\nu\eta\ln\rho + 2)}{\nu^2\eta\ln\rho}. \tag{37}$$

**8:** If $\nu = A, \mu = AB, (B \neq 0)$ and $\zeta = 0$,

$$B_{32}(\eta) = \rho^{A\eta} - B. \tag{38}$$

**9:** If $\nu = \zeta = 0$,

$$B_{33}(\eta) = \mu\eta\ln\rho. \tag{39}$$

**10:** If $\nu = \mu = 0$,

$$B_{34}(\eta) = \frac{-1}{\zeta\eta\ln\rho}. \tag{40}$$

**11:** If $\mu = 0$ and $\nu \neq 0$,

$$B_{35}(\eta) = -\frac{p\nu}{\zeta\left(\cosh_\rho(\nu\eta) - \sinh_\rho(\nu\eta) + p\right)}, \tag{41}$$

$$B_{36}(\eta) = -\frac{\nu\left(\cosh_\rho(\nu\eta) + \sinh_\rho(\nu\eta)\right)}{\zeta\left(\cosh_\rho(\nu\eta) + \sinh_\rho(\nu\eta) + q\right)}. \tag{42}$$

**12:** If $\zeta = AB,\ \nu = A\ $ ($\mu = 0$ and $B \neq 0$),

$$B_{37}(\eta) = -\frac{p\rho^{A\eta}}{p - Bq\rho^{A\eta}}. \tag{43}$$

**Note**
The generalized hyperbolic and triangular functions [30,31] are defined as follows:

$$\sinh_\rho(\eta) = \frac{p\rho^\eta - q\rho^{-\eta}}{2}, \qquad \cosh_\rho(\eta) = \frac{p\rho^\eta + q\rho^{-\eta}}{2},$$

$$\tanh_\rho(\eta) = \frac{p\rho^\eta - q\rho^{-\eta}}{p\rho^\eta + q\rho^{-\eta}}, \qquad \coth_\rho(\eta) = \frac{p\rho^\eta + q\rho^{-\eta}}{p\rho^\eta - q\rho^{-\eta}},$$

$$\mathrm{sech}_\rho(\eta) = \frac{2}{p\rho^\eta + q\rho^{-\eta}}, \qquad \mathrm{csch}_\rho(\eta) = \frac{2}{p\rho^\eta - q\rho^{-\eta}},$$

$$\sin_\rho(\eta) = \frac{p\rho^{\mathrm{i}\eta} - q\rho^{-\mathrm{i}\eta}}{2i}, \qquad \cos_\rho(\eta) = \frac{p\rho^{\mathrm{i}\eta} + q\rho^{-\mathrm{i}\eta}}{2},$$

$$\tan_\rho(\eta) = -\mathrm{i}\frac{p\rho^{\mathrm{i}\eta} - q\rho^{-\mathrm{i}\eta}}{p\rho^{\mathrm{i}\eta} + q\rho^{-\mathrm{i}\eta}}, \qquad \cot_\rho(\eta) = \mathrm{i}\frac{p\rho^{\mathrm{i}\eta} + q\rho^{-\mathrm{i}\eta}}{p\rho^{\mathrm{i}\eta} - q\rho^{-\mathrm{i}\eta}},$$

$$\sec_\rho(\eta) = \frac{2}{p\rho^\eta + q\rho^{-\eta}}, \qquad \csc_\rho(\eta) = \frac{2\mathrm{i}}{p\rho^\eta - q\rho^{-\eta}},$$

where $\eta$ is an independent variable and $p, q$ are non-zero arbitrary constants, called deformation parameters.
**Step 3:** After substituting the wave transformation in the considered NLPDE we will get the ordinary differential equation (ODE). By equalizing the highest order derivative with the nonlinear component of that ODE, we can obtain the balancing integer $N > 0$. Then, by replacing Eq. (5) in Eq. (4) we get the algebraic equations having powers of $B^j(\eta)$ $(j = 0, 1, 2, ...)$ and equating the coefficients of powers of $B(\eta)$ to zero gives an algebraic system of equations.
**Step 4:** Solve the algebraic system of equations and use the results in Eq. (5) to determine the exact solutions of Eq. (2).

## 3. Execution of the proposed methodology

In this section, we have applied the extended direct algebraic method on Eq. (1). By substituting the transformation from Eq. (3) into Eq. (1) we get the real part of the equation:

$$d_2^2(a+\delta)W''(\eta) + \alpha W^{2n+1}(\eta) + \beta W^{4n+1}(\eta) - (ad_1^2 - c_1 + \epsilon)W(\eta) = 0, \tag{44}$$

and imaginary part:

$$2(ad_1d_2 - c_2)W'(\eta) = 0, \quad \implies c_2 = 2ad_1d_2. \tag{45}$$

To find the balancing coefficient of the equation we will use the following transformation [23]:

$$W(\eta) = (w(\eta))^{\frac{1}{2n}}. \tag{46}$$

Eq. (44) converts to:

$$2nd_2^2(a+\delta)w(\eta)w''(\eta) + d_2^2(a+\delta)(1-2n)(w'(\eta))^2 + 4\alpha n^2w^3(\eta) + 4\beta n^2w^4(\eta) - 4n^2(ad_1^2 - c_1 + \epsilon)w^2(\eta) = 0. \tag{47}$$

So, by equating the nonlinear component $w^4(\eta)$ with the highest order derivative term $w(\eta)w''(\eta)$ balancing coefficient, $N = 1$ can be found. Then from Eq. (5) solution of Eq. (47) can be supposed as:

$$w(\eta) = b_0 + b_1B(\eta). \tag{48}$$

By putting Eq. (48) into Eq. (47) along with Eq. (6) and setting the coefficients of powers of $B^j(\eta)$ for $j = 0, 1, 2, 3, 4$ to $0$, we acquire the system of algebraic equations. Resolving the system of equations, we have obtained the following sets of solutions for the specific parametric values:
**Set 1:**

$$\alpha = \frac{-2n(n+1)(ad_1^2 - c_1 + \epsilon)}{b_0},$$

$$\beta = \frac{-n^2(2nad_1^2 - c_1 + \epsilon + ad_1^2 - 2nc_1 + 2n\epsilon)}{b_0^2},$$

$$\delta = -a + \frac{1}{\zeta\mu d_2^2 \ln(\rho)^2}(4n^4c_1 + 4n^3c_1 - 4n^4\epsilon - 4n^3\epsilon - 4n^4ad_1^2 - 4n^3ad_1^2),$$

$$\nu = \pm\frac{(1+2n)\zeta}{n\sqrt{\frac{\zeta(n+1)}{n\mu}}}, \qquad b_0 = b_0, \qquad b_1 = \pm b_0\sqrt{\frac{\zeta(n+1)}{n\mu}}.$$

**Set 2:**

$$\alpha = \frac{2\zeta(\pm n \pm 1)(ad_1^2 - c_1 + \epsilon)}{b_1\sqrt{\nu^2 - 4\mu\zeta}},$$

$$\beta = \frac{\zeta^2\left(2\,and_1{}^2 + ad_1{}^2 + 2\,n\epsilon - 2\,nc_1 + \epsilon - c_1\right)}{b_1{}^2\,(4\,(\zeta)\,\mu - \nu^2)},$$

$$\delta = -a - \frac{4\,n^2ad_1{}^2 + 4\,n^2\epsilon - 4\,n^2c_1}{d_2{}^2\,(\ln(\rho))^2\,(4\,(\zeta)\,\mu - \nu^2)},$$

$$b_0 = b_1\left(\frac{\nu \pm \sqrt{\nu^2 - 4\mu\zeta}}{2\zeta}\right), \qquad b_1 = b_1.$$

### 3.1. Solutions of Eq. (1) by using Set 1

By utilizing the values from Set 1 in Eq. (48) and doing backward substitution we have the following solutions for over wave profile.

**Case 2:** If $\Theta > 0$ and $\zeta \neq 0$,

$$\phi_6 = \exp \mathrm{i}(d_1 x - c_1 t)\left[b_0\left(1 \pm \frac{m}{2\sqrt{\mu\zeta}}(\nu + \sqrt{\Theta}\tanh_\rho(\frac{\sqrt{\Theta}}{2}\eta))\right)\right]^{\frac{1}{2n}},$$

$$\phi_7 = \exp \mathrm{i}(d_1 x - c_1 t)\left[b_0\left(1 \pm \frac{m}{2\sqrt{\mu\zeta}}(\nu + \sqrt{\Theta}\coth_\rho(\frac{\sqrt{\Theta}}{2}\eta))\right)\right]^{\frac{1}{2n}},$$

$$\phi_8 = \exp \mathrm{i}(d_1 x - c_1 t)\left[b_0 \pm \frac{b_0 m}{2\sqrt{\mu\zeta}}\left(\nu - \sqrt{\Theta}(-\tanh_\rho(\sqrt{\Theta}\eta) \pm \mathrm{i}\sqrt{pq}\,\mathrm{sech}_\rho(\sqrt{\Theta}\eta))\right)\right]^{\frac{1}{2n}},$$

$$\phi_9 = \exp \mathrm{i}(d_1 x - c_1 t)\left[b_0 \pm \frac{b_0 m}{2\sqrt{\mu\zeta}}\left(\nu - \sqrt{\Theta}(-\coth_\rho\left(\sqrt{\Theta}\eta\right) \pm \sqrt{pq}\,\mathrm{csch}_\rho\left(\sqrt{\Theta}\eta\right))\right)\right]^{\frac{1}{2n}},$$

$$\phi_{10} = \exp \mathrm{i}(d_1 x - c_1 t)\left[b_0 \pm \frac{b_0 m}{4\sqrt{\mu\zeta}}\left(2\nu + \sqrt{\Theta}(\tanh_\rho(\frac{\sqrt{\Theta}}{4}\eta) + \coth_\rho(\frac{\sqrt{\Theta}}{4}\eta))\right)\right]^{\frac{1}{2n}}.$$

**Case 9:** If $\nu = \zeta = 0$,

$$\phi_{33} = b_0.$$

Here, $m = \sqrt{n + 1/n}$. We can see that only the above cases are valid for the parameters involved in Set 1 because conditions of other cases fail to satisfy the value of $\nu$.

### 3.2. Solutions of Eq. (1) by using Set 2

In this subsection, we have used Set 2 in Eq. (48) then the formed solution has been substituted in Eq. (47). Afterward, with the help of Eq. (46), Eq. (44), and transformation in Eq. (3) we get the following solutions of considered complex-valued function.

**Case 2:** If $\Theta > 0$ and $\zeta \neq 0$,

$$\phi_6 = \exp \mathrm{i}(d_1 x - c_1 t)\left[b_1\left(\pm\frac{\sqrt{\Theta}}{2\zeta} - \frac{\sqrt{\Theta}}{2\zeta}\tanh_\rho(\frac{\sqrt{\Theta}}{2}\eta)\right)\right]^{\frac{1}{2n}},$$

$$\phi_7 = \exp \mathrm{i}(d_1 x - c_1 t)\left[b_1\left(\pm\frac{\sqrt{\Theta}}{2\zeta} - \frac{\sqrt{\Theta}}{2\zeta}\coth_\rho(\frac{\sqrt{\Theta}}{2}\eta)\right)\right]^{\frac{1}{2n}},$$

$$\phi_8 = \exp \mathrm{i}(d_1 x - c_1 t)\left[\pm\frac{b_1\sqrt{\Theta}}{2\zeta} + \frac{b_1\sqrt{\Theta}}{2\zeta}(-\tanh_\rho(\sqrt{\Theta}\eta) \pm \mathrm{i}\sqrt{pq}\,\mathrm{sech}_\rho(\sqrt{\Theta}\eta))\right]^{\frac{1}{2n}},$$

$$\phi_9 = \exp \mathrm{i}(d_1 x - c_1 t)\left[\pm\frac{b_1\sqrt{\Theta}}{2\zeta} + \frac{b_1\sqrt{\Theta}}{2\zeta}(-\coth_\rho\left(\sqrt{\Theta}\eta\right) \pm \sqrt{pq}\,\mathrm{csch}_\rho\left(\sqrt{\Theta}\eta\right))\right]^{\frac{1}{2n}},$$

$$\phi_{10} = \exp \mathrm{i}(d_1 x - c_1 t)\left[\pm\frac{b_1\sqrt{\Theta}}{2\zeta} - \frac{b_1\sqrt{\Theta}}{4\zeta}(\tanh_\rho(\frac{\sqrt{\Theta}}{4}\eta) + \coth_\rho(\frac{\sqrt{\Theta}}{4}\eta))\right]^{\frac{1}{2n}}.$$

**Case 4:** If $\mu\zeta < 0$ and $\nu = 0$,

$$\phi_{16} = \exp \mathrm{i}(d_1x - c_1t)\Bigg[\pm \frac{b_1\sqrt{-\mu\zeta}}{\zeta} - b_1\sqrt{-\frac{\mu}{\zeta}}\tanh_\rho\left(\sqrt{-\mu\zeta}\eta\right)\Bigg]^{\frac{1}{2n}},$$

$$\phi_{17} = \exp \mathrm{i}(d_1x - c_1t)\Bigg[\pm \frac{b_1\sqrt{-\mu\zeta}}{\zeta} - b_1\sqrt{-\frac{\mu}{\zeta}}\coth_\rho\left(\sqrt{-\mu\zeta}\eta\right)\Bigg]^{\frac{1}{2n}},$$

$$\phi_{18} = \exp \mathrm{i}(d_1x - c_1t)\Bigg[\pm b_1\frac{\sqrt{-\mu\zeta}}{\zeta} - b_1\sqrt{\frac{\mu}{\zeta}}\Big(\mathrm{i}\tanh_\rho(2\sqrt{-\mu\zeta}\eta) \pm \sqrt{pq}\,\mathrm{sech}_\rho(2\sqrt{-\mu\zeta}\eta)\Big)\Bigg]^{\frac{1}{2n}},$$

$$\phi_{19} = \exp \mathrm{i}(d_1x - c_1t)\Bigg[\pm b_1\frac{\sqrt{-\mu\zeta}}{\zeta} - b_1\mathrm{i}\sqrt{\frac{\mu}{\zeta}}\Big(\coth_\rho(2\sqrt{-\mu\zeta}\eta) \pm \sqrt{pq}\,\mathrm{csch}_\rho(2\sqrt{-\mu\zeta}\eta)\Big)\Bigg]^{\frac{1}{2n}},$$

$$\phi_{20} = \exp \mathrm{i}(d_1x - c_1t)\Bigg[\pm b_1\frac{\sqrt{-\mu\zeta}}{\zeta} - \frac{b_1}{2}\sqrt{-\frac{\mu}{\zeta}}\Big(\tanh_\rho(\frac{\sqrt{-\mu\zeta}}{2}\eta) + \coth_\rho(\frac{\sqrt{-\mu\zeta}}{2}\eta)\Big)\Bigg]^{\frac{1}{2n}}.$$

**Case 6:** If $\nu = 0$ and $\zeta = -\mu$,

$$\phi_{26} = \exp \mathrm{i}(d_1x - c_1t)\Big[b_1\left(\pm 1 - \tanh_\rho(\mu\eta)\right)\Big]^{\frac{1}{2n}},$$

$$\phi_{27} = \exp \mathrm{i}(d_1x - c_1t)\Big[b_1\left(\pm 1 - \coth_\rho(\mu\eta)\right)\Big]^{\frac{1}{2n}},$$

$$\phi_{28} = \exp \mathrm{i}(d_1x - c_1t)\Big[\pm b_1 - b_1 tanh_\rho(2\mu\eta) \pm b_1\sqrt{-pq}\,\mathrm{sech}_\rho(2\mu\eta)\Big]^{\frac{1}{2n}},$$

$$\phi_{29} = \exp \mathrm{i}(d_1x - c_1t)\Big[\pm b_1 - b_1\coth_\rho(2\mu\eta) \pm b_1\sqrt{pq}\,\mathrm{csch}_\rho(2\mu\eta)\Big]^{\frac{1}{2n}},$$

$$\phi_{30} = \exp \mathrm{i}(d_1x - c_1t)\Bigg[\pm b_1 - \frac{b_1}{2}\Big(\tanh_\rho(\frac{\mu}{2}\eta) + \coth_\rho(\frac{\mu}{2}\eta)\Big)\Bigg]^{\frac{1}{2n}}.$$

**Case 11:** If $\mu = 0$ and $\nu \neq 0$,

$$\phi_{35} = \exp \mathrm{i}(d_1x - c_1t)\Bigg[-\frac{b_1p\nu}{\zeta\Big(\cosh_\rho(\nu\eta) - \sinh_\rho(\nu\eta) + p\Big)}\Bigg]^{\frac{1}{2n}},$$

$$\phi_{36} = \exp \mathrm{i}(d_1x - c_1t)\Bigg[-\frac{b_1\nu\Big(\cosh_\rho(\nu\eta) + \sinh_\rho(\nu\eta)\Big)}{\zeta\Big(\cosh_\rho(\nu\eta) + \sinh_\rho(\nu\eta) + q\Big)}\Bigg]^{\frac{1}{2n}}.$$

**Case 12:** If $\zeta = AB,\ \nu = A(\mu = 0$ and $B \neq 0)$,

$$\phi_{37} = \exp \mathrm{i}(d_1x - c_1t)\left[\frac{b_1}{2B} \pm \frac{b_1}{2B} - \frac{b_1p\rho^{A\eta}}{p - Bq\rho^{A\eta}}\right]^{\frac{1}{2n}}.$$

It can be seen that the other cases presented in Sec. 2 do not give solutions for the values of parameters given in Set 2.

### 3.3. Physical appraisal for solutions in set 2

Graphs have long been the primary way to visually represent data connections. This section contains several graphs of the absolute solutions represented in set 2 that reflect the exact soliton structures of the model specified in Eq. (1). In the presence of physical factors, figures featuring the behavior of solitons have been shown in the range $(-10, 10)$. The results of our solutions will be in the form of nonlinear pulses.

Figure 1 shows a dark kink-type solitary wave for certain values of parameters involved in $|\phi_6|$. It can be observed that the soliton communicates its pattern and intensity in a uniform manner.

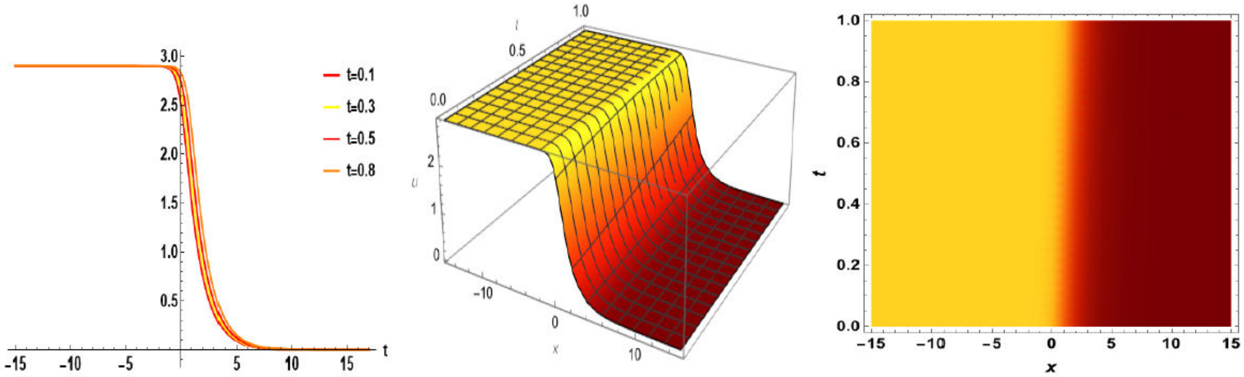


a) 2D-Plot of $|\phi_6|$ b) 3D-Plot of $|\phi_6|$ c) 2D-Contour of $|\phi_6|$

FIGURE 1. Graphical representations of $|\phi_6|$ for parameters $d_1 = d_2 = c_1 = c_2 = 1,\ b_0 = 25, \nu = 4,\ \rho = e, n = 2,\ \mu = 2,\ \zeta = 1$ and $\Theta = 8$.

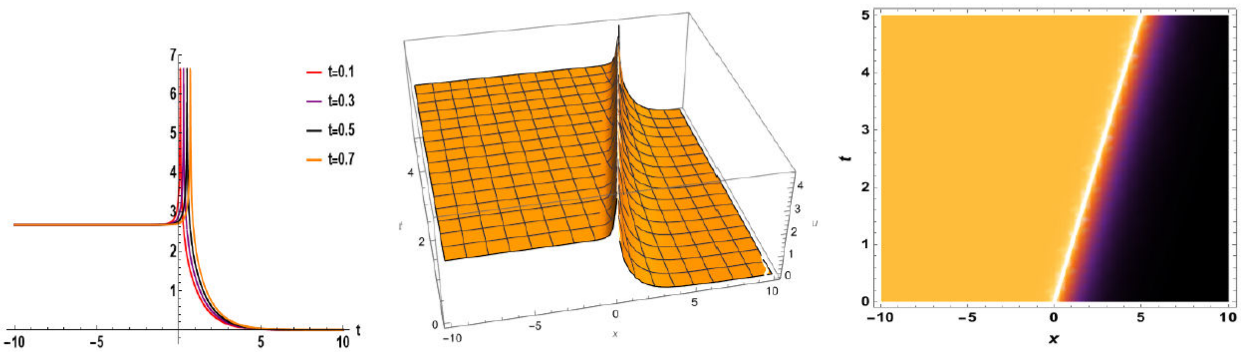


a) 2D-Plot of $|\phi_{27}|$ b) 3D-Plot of $|\phi_{27}|$ c) 2D-Contour of $|\phi_{27}|$

FIGURE 2. Graphical representations of $|\phi_{27}|$ for parameters $d_1 = d_2 = c_1 = c_2 = 1,\ b_0 = 25, \nu = 0,\ \rho = e, n = 2,\ \mu = 2,\ \zeta = -2$.

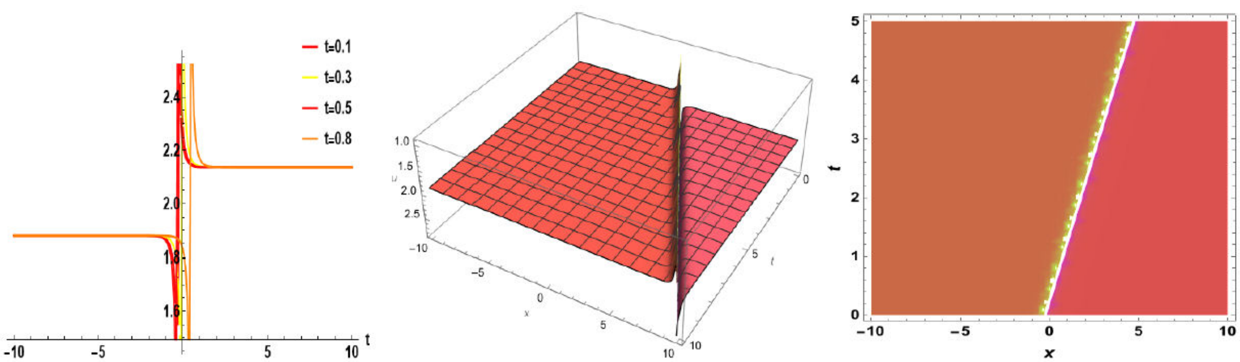


a) 2D-Plot of $|\phi_{37}|$ b) 3D-Plot of $|\phi_{37}|$ c) 2D-Contour of $|\phi_{37}|$

FIGURE 3. Graphical representations of $|\phi_{37}|$ for parameters $d_1 = d_2 = c_1 = c_2 = 1,\ b_0 = 25, \nu = 4,\ \rho = e, n = 2,\ \zeta = 8$ and $p = 2,\ q = 3$.

Figure 2 shows the propagation of a bright solitary wave for different values of the parameters involved. We can observe from these graphs that the amplitude of the wave becomes constant after a certain point.

Figure 3 gives us a visual of a singular kink solution for different parametric values of $|\phi_{37}|$ having specific shapes and intensity.

## 4. Bifurcation behavior and phase portraits

In this section, the bifurcation of the underlying equation is addressed [33-35]. In order to accomplish our objective, we transformed the nonlinear partial differential equation under consideration into an ordinary differential equation by using the traveling wave transformation that was previously discussed in Eq. (47).

The following planer dynamical system has been established using Eq. (47):

$$\begin{cases} w^{'}(\eta) = z(\eta), \\ z^{'} = \frac{-[\psi_2 z^2+\psi_3 w^4+\psi_4 w^3+\psi_5 w^2]}{\psi_1 w}, \end{cases} \quad (49)$$

where, $\psi_1 = d_2^2(a+\delta), \psi_2 = d_2^2(a+\delta)(1-2n), \psi_3 = 4\beta n^2, \psi_4 = 4\alpha n^2, \psi_5 = -4n^2(ad_1^2 - c_1 + \epsilon)$. Clearly, this system is not a Hamiltonian system because the term $1/\psi_1 w$ in the second equation complicates the expression, as Hamiltonian systems usually involve linear and straightforward relationships in their partial derivatives. Also, the structure of the second differential equation does not align with the standard form of Hamiltonian dynamics. From (49), we have

$$\frac{dz^2}{dw} = \frac{-2[\psi_2 z^2+\psi_3 w^4+\psi_4 w^3+\psi_5 w^2]}{\psi_1 w}, \quad (50)$$

since $w=0$ is a singular point of the above equation, only certain specific circumstances could lead $w$ to zero. The solution to Eq. (50) is presented by

$$z^2 = -\frac{\psi_3 w^4}{2\psi_1+\psi_2} - \frac{2\psi_4 w^3}{3\psi_1+2\psi_2} - \frac{\psi_5 w^2}{\psi_1+\psi_2} + \mathcal{C}_1 w^{-\frac{2\psi_2}{\psi_1}}, \quad (51)$$

when $\psi_2 \neq 0$, and

$$z^2 = -\frac{\psi_3 w^4}{2\psi_1} - \frac{2\psi_4 w^3}{3\psi_1} - \frac{\psi_5 w^2}{\psi_1} + \mathcal{C}_1^{'}, \quad (52)$$

when $\psi_2 = 0$. Then we have

$$(w^{'})^2 + \frac{\psi_3 w^4}{2\psi_1+\psi_2} + \frac{2\psi_4 w^3}{3\psi_1+2\psi_2} + \frac{\psi_5 w^2}{\psi_1+\psi_2} - \mathcal{C}_1 w^{-\frac{2\psi_2}{\psi_1}} = 0, \qquad (\psi_2 \neq 0), \quad (53)$$

and

$$(w^{'})^2 + \frac{\psi_3 w^4}{2\psi_1} + \frac{2\psi_4 w^3}{3\psi_1} + \frac{\psi_5 w^2}{\psi_1} - \mathcal{C}_1^{'} = 0, \quad (\psi_2 = 0), \quad (54)$$

where $\mathcal{C}_1$ and $\mathcal{C}_1^{'}$ are constants of integration. The following conserved quantity could be obtained:

$$H(w,z) = z^2 + \frac{\psi_3 w^4}{2\psi_1+\psi_2} + \frac{2\psi_4 w^3}{3\psi_1+2\psi_2} + \frac{\psi_5 w^2}{\psi_1+\psi_2} - \mathcal{C}_1 w^{-\frac{2\psi_2}{\psi_1}}, \qquad (\psi_2 \neq 0), \quad (55)$$

and

$$H(w,z) = z^2 + \frac{\psi_3 w^4}{2\psi_1} + \frac{2\psi_4 w^3}{3\psi_1} + \frac{\psi_5 w^2}{\psi_1} - \mathcal{C}_1^{'}, \quad (\psi_2 = 0), \quad (56)$$

which are undoubtedly conserved quantities. Since both Eq. (55) and Eq. (56) are autonomous, their global phase portraits are merely their contour lines. The complete discriminating system is introduced in the section that follows, where we then undertake a qualitative analysis based on this issue. Since resolving Eq. (53) as a whole is extremely challenging, we simply concentrate on the scenario where $\psi_2/\psi_1 = -1/2$, and similar discussions could take place for other conditions such as $\psi_2/\psi_1 = -3/4$ and $\psi_2/\psi_1 = -5/6$.

We take into account two cases, where $\mathcal{C}_1$ is either not equal to zero or zero, respectively.

**Case 1:** If $\mathcal{C}_1 \neq 0$, $\psi_2/\psi_1 = -1/2$, then Eq. (55) becomes

$$H(w,z) = z^2 + \frac{\psi_3 w^4}{2\psi_1+\psi_2} + \frac{2\psi_4 w^3}{3\psi_1+2\psi_2} + \frac{\psi_5 w^2}{\psi_1+\psi_2} - \mathcal{C}_1 w, \quad (57)$$

with its potential energy given by

$$U(w) = \frac{\psi_3 w^4}{2\psi_1+\psi_2} + \frac{2\psi_4 w^3}{3\psi_1+2\psi_2} + \frac{\psi_5 w^2}{\psi_1+\psi_2} - \mathcal{C}_1 w, \quad (58)$$

and thus we have

$$U^{'}(w) = \frac{4\psi_3 w^3}{2\psi_1+\psi_2} + \frac{6\psi_4 w^2}{3\psi_1+2\psi_2} + \frac{2\psi_5 w}{\psi_1+\psi_2} - \mathcal{C}_1 = g_1 w^3 + g_2 w^2 + g_3 w - \mathcal{C}_1, \quad (59)$$

where

$$g_1 = \frac{4\psi_3}{2\psi_1+\psi_2}, \qquad g_2 = \frac{6\psi_4}{3\psi_1+2\psi_2},$$

and

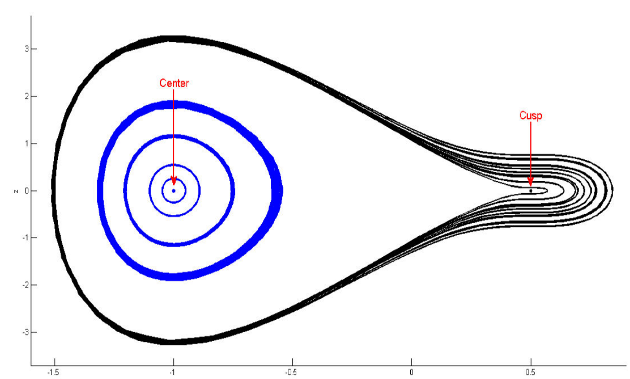


FIGURE 4. The equilibrium points of Eq. (62), at $s = 0.5$ as cuspidal point presented in blue and $p = -1$ as center point in black color.

$$g_3 = \frac{2\psi_5}{\psi_1 + \psi_2}.$$

By denoting

$$J(w,z) = \begin{vmatrix} 0 & 1 \\ 3g_1w^2 + 2g_2w + g_3 & 0 \end{vmatrix}$$
$$= -(3g_1w^2 + 2g_2w + g_3), \qquad (60)$$

for $J(w,z) < 0$, $(w,0)$ is a saddle point; for $J(w,z) > 0$, it is a center; and for $J(w,z) = 0$, it is a cuspidal point.

Inaugurating the third-order discriminant to the polynomial given in Eq. (59),

$$\Delta_3 = g_2^2g_3^2 - 4g_1g_3^3 + 4g_2^3\mathcal{C}_1 - 27g_1^2\mathcal{C}_1^2 - 18g_1g_2g_3\mathcal{C}_1. \qquad (61)$$

The outcomes that we can get are as follows:

**Case 1.1:** For $\Delta = 0$, $g_1 < 0$, $g_2 = 0$, $g_3 > 0$ and $c_1 > 0$, we have

$$U^{'}(w) = (w-s)^2(w-p), \quad (2s+p=0), \qquad (62)$$

where $(s,0)$ is a cuspidal point and $(p,0)$ is a center depicted in Fig. 4. For $g_1 = -12$, $g_2 = 0$, $g_3 = 9$ and $c_1 = 3$, the equilibrium points are $s = 0.5$ and $p = -1$.

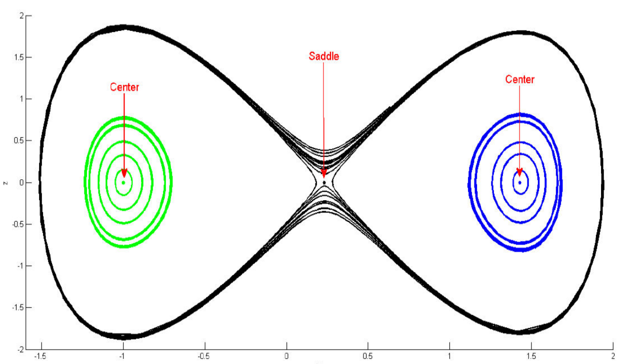


FIGURE 5. The equilibrium points of Eq. (63), at $s = -1$, $p = 1.43$ as center points presented in blue and green colors and $q = 0.23$ as saddle point in black color.

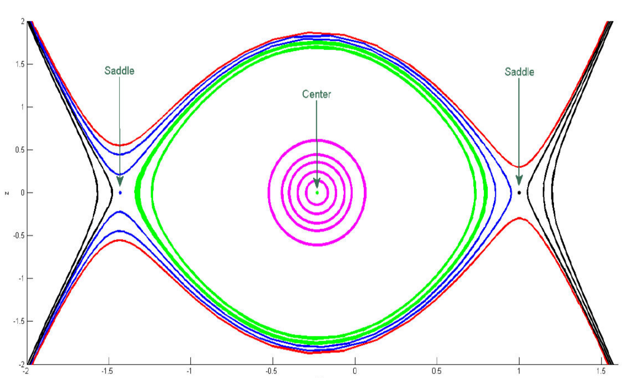


FIGURE 6. The equilibrium points of Eq. (64), at $s = 1$, $p = -1.43$ as saddle points presented by multi colors and $q = -0.23$ as center point in purple color.

**Case 1.2:** $\Delta > 0$, $g_1 < 0$, $g_2 > 0$, $g_3 > 0$ and $c_1 > 0$, we have

$$U^{'}(w) = (w-s)(w-p)(w-q), \qquad (63)$$

where $(s,0)$ and $(p,0)$ are centers and $(q,0)$ represents a saddle point represented in Fig. 5. For $g_1 = -3$, $g_2 = 2$, $g_3 = 4$ and $c_1 = 1$, the equilibrium points are $s = -1$, $q = 0.23$ and $p = 1.43$.

**Case 1.3:** $\Delta > 0$, $g_1 > 0$, $g_2 > 0$, $g_3 < 0$ and $c_1 > 0$, we have

$$U^{'}(w) = (w-s)(w-p)(w-q), \qquad (64)$$

where the points $(s,0)$, $(p,0)$ act as saddle points and $(q,0)$ represents a center shown in Fig. 6. For $g_1 = 3$, $g_2 = 2$, $g_3 = -4$ and $c_1 = 1$, the equilibrium points are $s = 1$, $q = -0.23$ and $p = -1.43$.

**Case 1.4:** $\Delta < 0$, $g_1 > 0$, $g_2 > 0$, $g_3 > 0$ and $c_1 < 0$, we have

$$U^{'}(w) = (w-s)[(w-p)^2 + q^2]. \qquad (65)$$

Here, $(s,0)$ is the only real equilibrium point, and it is a saddle point as can be seen in Fig. 7. For $g_1 = 8$, $g_2 = 2$, $g_3 = 1$ and $c_1 = -1$, the only real equilibrium point is $s = -1/2$.

**Case 2:** $\mathcal{C}_1 = 0$, $\psi_2/\psi_1 = -1/2$. In this case, we rewrite Eq. (55) in the form

$$H(w,z) = z^2 + \frac{\psi_3w^4}{2\psi_1 + \psi_2} + \frac{2\psi_4w^3}{3\psi_1 + 2\psi_2} + \frac{\psi_5w^2}{\psi_1 + \psi_2}, \qquad (66)$$

with its potential energy given by

$$P(w) = \frac{\psi_3w^4}{2\psi_1 + \psi_2} + \frac{2\psi_4w^3}{3\psi_1 + 2\psi_2} + \frac{\psi_5w^2}{\psi_1 + \psi_2}, \qquad (67)$$

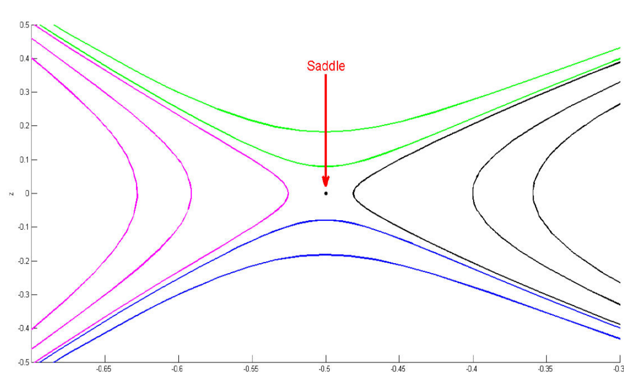


FIGURE 7. The equilibrium point of Eq. (65), at $s = -0.5$ as saddle point.

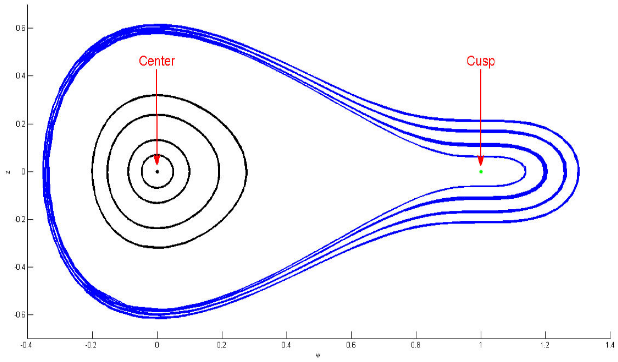


FIGURE 8. The equilibrium points of Eq. (70), at $s = 1$ as cuspidal point presented in blue and $l = 1$ as center point in black color.

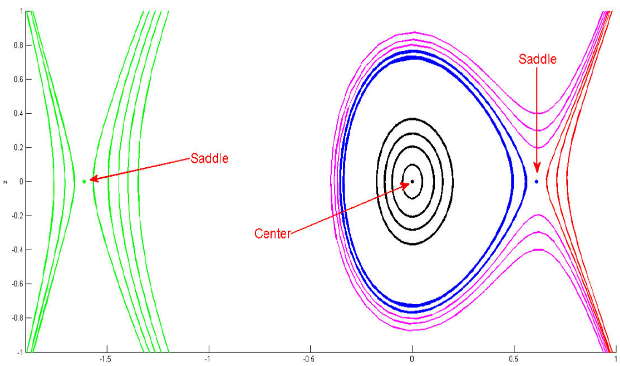


FIGURE 9. The equilibrium points of Eq. (71), at $s = 0.61$, $l = -1.61$ as saddle points presented in green and other colors and $m = 0$ as center point in black color.

and thus we have

$$P^{'}(w) = \frac{4\psi_3 w^3}{2\psi_1 + \psi_2} + \frac{6\psi_4 w^2}{3\psi_1 + 2\psi_2} + \frac{2\psi_5 w}{\psi_1 + \psi_2}$$
$$= g_1 w^3 + g_2 w^2 + g_3 w. \tag{68}$$

With discriminant:

$$\Delta_3 = g_2^2 g_3^2 - 4 g_1 g_3^3, \tag{69}$$

The preceding outcomes are possible.
**Case 2.1:** $\Delta = 0$, $g_1 < 0$, $g_2 > 0$, and $g_3 < 0$, we have

$$P^{'}(w) = (w - s)^2 (w - l), \tag{70}$$

where $(s, 0)$ and $(l, 0)$ are cuspidal and center points respectively, depicted in Fig. 8. For $g_1 = -2$, $g_2 = 4$ and $g_3 = -2$, the equilibrium points are $s = 1$ and $l = 1$.
**Case 2.2** $\Delta > 0$, $g_1 > 0$, $g_2 > 0$ and $g_3 < 0$, we get

$$U^{'}(w) = (w - s)(w - l)(w - m), \tag{71}$$

where $(s, 0)$ and $(l, 0)$ act as saddle points with $(m, 0)$ representing a center shown in Fig. 9. For $g_1 = 4$, $g_2 = 4$ and $g_3 = -4$, the equilibrium points are $s = 0.61$, $m = 0$ and $l = -1.61$.

## 5. Conclusion

In this study, novel soliton solutions to the generalized resonant nonlinear Schrödinger problem were constructed using the proposed extended direct algebraic approach. Since this equation cannot be integrated, we searched for solutions to this model by using the traveling wave reductions, after which various structures such as dark, bright, and singular kink-type solitary waves were revealed. These built solutions aid in the understanding of complicated physical phenomena and have applications in optical fibers and transmission lines. These propagating waves were also shown by contour and multidimensional graphs. Bifurcation analysis of the considered system have also been discussed. The system was first turned into a planar dynamical system, and subsequently into a Hamiltonian system. Using the discriminant, the instances were then predicted and effectively shown in the phase portrait. Additionally, the accuracy of the solutions has been verified using a computer software package. These findings serve as a pillar of encouragement for further research in this area.


## Acknowledgements

This work was supported and funded by the Deanship of Scientific Research at Imam Mohammad Ibn Saud Islamic University (IMSIU) (grant number IMSIU-DDRSP2501). The authors are thankful to the anonymous reviewers for providing valuable suggestions that improve the overall quality of the paper.



1. H. Jin *et al.*, A hypothetical learning progression for quantifying phenomena in science, *Science and Education* **28** (2019) 1181, `https://doi.org/10.1007/s11191-019-00076-8`.
2. J. X. Yao, Y. Y. Guo, and K. Neumann, Towards a hypothetical learning progression of scientific explanation, *Asia-Pacific science education* **2** (2016) 1, `https://doi.org/10.1186/s41029-016-0011-7`.
3. A. Hasegawa, Optical solitons in fibers (Springer Science and Business Media, 2013). `https://doi.org/10.1007/BFb0041284`.
4. A. A. Sukhorukov *et al.*, Spatial optical solitons in waveguide arrays, *IEEE Journal of quantum electronics* **39** (2003) 31, `https://doi.org/10.1109/JQE.2002.806184`.
5. C. Spiess *et al.*, Chirped dissipative solitons in driven optical resonators, *Optica* **8** (2021) 861, `https://doi.org/10.1364/OPTICA.419771`.
6. P. Kaur, D. Dhawan, and N. Gupta, Review on optical soli-

tons for long haul transmission, *Journal of Optical Communications* **45** (2023) 1, https://doi.org/10.1515/joc-2023-0093.

7. H. S. Eisenberg *et al*., Discrete spatial optical solitons in waveguide arrays, *Physical Review Letters* **81** (1998) 3383, https://doi.org/10.1103/PhysRevLett.81.3383.
8. A. Biswas, Quasi-stationary optical solitons with parabolic law nonlinearity, *Optics communications* **216** (2003) 427, https://doi.org/10.1016/S0030-4018(02)02309-X.
9. F. Ali *et al*., Solitonic, quasi-periodic, super nonlinear and chaotic behaviors of a dispersive extended nonlinear Schrödinger equation in an optical fiber, *Results in Physics* **31** (2021) 104921, https://doi.org/10.1016/j.rinp.2021.104921.
10. N. Raza, S. Arshed, and A. Javid, Optical solitons and stability analysis for the generalized second-order nonlinear Schrödinger equation in an optical fiber, *International Journal of Nonlinear Sciences and Numerical Simulation* **21** (2020) 855, https://doi.org/10.1515/ijnsns-2019-0287.
11. N. Raza *et al*., Optical solitons and stability regions of the higher order nonlinear Schrödinger's equation in an inhomogeneous fiber, *International Journal of Nonlinear Sciences and Numerical Simulation* **24** (2021) 1. https://doi.org/10.1515/ijnsns-2021-0165.
12. N. Raza, M. R. Aslam, and H. Rezazadeh, Analytical study of resonant optical solitons with variable coefficients in Kerr and non-Kerr law media, *Optical and Quantum Electronics* **51** (2019) 1, https://doi.org/10.1007/s11082-019-1773-4.
13. L. Akinyemi *et al*., Nonlinear dispersion in parabolic law medium and its optical solitons, *Results in Physics* **26** (2021) 104411, https://doi.org/10.1016/j.rinp.2021.104411.
14. A. Jhangeer, H. Almusawa, and Z. Hussain, Bifurcation study and pattern formation analysis of a non-linear dynamical system for chaotic behavior in travelling wave solution, *Results in Physics* (2022) 105492, https://doi.org/10.1016/j.rinp.2022.105492.
15. M. Arshad, A. R. Seadawy, and D. Lu, Exact bright-dark solitary wave solutions of the higher-order cubic-quintic nonlinear Schrödinger equation and its stability, *Optik* **138** (2017) 40, https://doi.org/10.1016/j.ijleo.2017.03.005.
16. S. Pathania *et al*., Chirped nonlinear resonant states in femtosecond fiber optics, *Optik* **227** (2021) 166094, https://doi.org/10.1016/j.ijleo.2020.166094.
17. S. Meradjia *et al*., Chirped self-similar cnoidal waves and similaritons in an inhomogeneous optical medium with resonant nonlinearity, *Chaos Solitons Fractals* **141** (2020) 110441, https://doi.org/10.1016/j.chaos.2020.110441.
18. M. Eslami, M. Mirzazadeh, and A. Biswas, Soliton solutions of the resonant nonlinear Schrödinger's equation in optical fibers with time-dependent coefficients by simplest equation approach, *J. Modern Opt*. **60** (2013) 1627, https://doi.org/10.1080/09500340.2013.850777.
19. A. R. Seadawy *et al*., Conservation laws and optical solutions of the resonant nonlinear Schrödinger's equation with parabolic nonlinearity, *Optik* **225** (2021) 165762, https://doi.org/10.1016/j.ijleo.2020.165762.
20. H. Triki *et al*., Bright and dark solitons for the resonant nonlinear Schrödinger's equation with time-dependent coefficients, *Optics and Laser Technology* **44** (2012) 2223, https://doi.org/10.1016/j.optlastec.2012.01.037.
21. F. Williams *et al*., Solitary waves in the resonant nonlinear Schrödinger equation: Stability and dynamical properties, *Physics Letters A* **22** (2020) 126441, https://doi.org/10.1016/j.physleta.2020.126441.
22. N. A. Kudryashov, Optical solitons of the resonant nonlinear Schrödinger equation with arbitrary index, *Optik* **235** (2021) 166626, https://doi.org/10.1016/j.ijleo.2021.166626.
23. K. S. Nisar *et al*., New solutions for the generalized resonant nonlinear Schrödinger equation, *Results in Physics* **33** (2022) 105153, https://doi.org/10.1016/j.rinp.2021.105153.
24. N. Raza and A. Zubair, Optical dark and singular solitons of generalized nonlinear Schrödinger's equation with anti-cubic law of nonlinearity, *Modern Physics Letters B* **33** (2019) 1950158, https://doi.org/10.1142/S0217984919501586.
25. N. Raza and A. Zubair, Bright, dark and dark-singular soliton solutions of nonlinear Schrödinger's equation with spatiotemporal dispersion, *Journal of Modern Optics* **65** (2018) 1975, https://doi.org/10.1080/09500340.2018.1480066.
26. N. Raza and Z. A. Alhussain, An explicit plethora of soliton solutions for a new microtubules transmission lines model: A fractional comparison, *Modern Physics Letters B* **35** (2021) 2150498, https://doi.org/10.1142/S0217984921504984.
27. A. R. Butt *et al*., Propagation of novel traveling wave envelopes of Zhiber-Shabat equation by using Lie analysis, International *Journal of Geometric Methods in Modern Physics* **20** (2023) 2350091, https://doi.org/10.1142/S0219887823500913.
28. C. Liu and Z. Li, The dynamical behavior analysis and the traveling wave solutions of the stochastic Sasa-Satsuma equation, *Qualitative Theory of Dynamical Systems* **23** (2024) 157, https://doi.org/10.1007/s12346-024-01022-y.
29. M. S. Ghayad *et al*., Derivation of optical solitons and other solutions for nonlinear Schrödinger equation using modified extended direct algebraic method, *Alexandria Engineering Journal* **64** (2023) 801, https://doi.org/10.1016/j.aej.2022.10.054.
30. M. A. Bashir and A. A. Moussa, The cotha ($\xi$) expansion method and its application to the Davey-Stewartson equation, *Applied Mathematical Sciences* **8** (2014) 3851, http://dx.doi.org/10.12988/ams.2014.45362.
31. Y. Ren and H. Zhang, New generalized hyperbolic functions and auto-Bäcklund transformation to find new exact solutions of the (2+1)-dimensional NNV equation, *Physics Letters A* **357** (2006) 438, https://doi.org/10.1016/j.physleta.2006.04.082.

32. S. Thota, An Introduction to Maple software (InNational Conference on Advances in Mathematical sciences, 2012), pp. 05-07.

33. A. Jhangeer *et al*., Nonlinear self-adjointness, conserved quantities, bifurcation analysis and travelling wave solutions of a family of long-wave unstable lubrication model, *Pramana* **94** (2020) 1, https://doi.org/10.1007/s12043-020-01961-6.

34. N. Raza *et al*., NDynamical analysis and phase portraits of two-mode waves in different media, *Results in Physics* **19** (2020) 103650, https://doi.org/10.1016/j.rinp.2020.103650.

35. A. Jhangeer *et al*., New exact solitary wave solutions, bifurcation analysis and first order conserved quantities of resonance nonlinear Schrödinger's equation with Kerr law nonlinearity, *Journal of King Saud University-Science* **33** (2021) 101180, https://doi.org/10.1016/j.jksus.2020.09.007.